BNWL-1025
~~UC-37~~
5-
4-69

[redacted]

ESTIMATED READOUT ERRORS PRODUCED BY RADIATION AND TEMPERATURE EFFECTS IN COAXIAL SIGNAL CABLES FOR FFTF

April 1969

[redacted]

AEC RESEARCH & DEVELOPMENT REPORT

BATTELLE NORTHWEST
BATTELLE MEMORIAL INSTITUTE
PACIFIC NORTHWEST LABORATORY
BATTELLE BOULEVARD, P. O. BOX 999, RICHLAND, WASHINGTON 99352

BNWL-1025

LEGAL NOTICE

PACIFIC NORTHWEST LABORATORY
RICHLAND, WASHINGTON
operated by
BATTELLE MEMORIAL INSTITUTE
for the
UNITED STATES ATOMIC ENERGY COMMISSION UNDER CONTRACT AT(45-1)-1830

AEC-RL RICHLAND, WASH.

BNWL-1025
UC-37, Instruments

ESTIMATED READOUT ERRORS PRODUCED BY RADIATION AND TEMPERATURE EFFECTS IN COAXIAL SIGNAL CABLES FOR FFTF

By

J. L. Stringer
R. R. Bourassa*

Applied Physics Department
Systems and Electronics Division

April 1969

BATTELLE MEMORIAL INSTITUTE
PACIFIC NORTHWEST LABORATORY
RICHLAND, WASHINGTON 99352

---

* *Present address: University of Oklahoma, Department of Physics, Norman, Oklahoma*

Printed in the United States of America
Available from
Clearinghouse for Federal Scientific and Technical Information
National Bureau of Standards, U.S. Department of Commerce
Springfield, Virginia 22151
Price: Printed Copy $3.00; Microfiche $0.65

ESTIMATED READOUT ERRORS PRODUCED BY RADIATION AND TEMPERATURE EFFECTS IN COAXIAL SIGNAL CABLES FOR FFTF

J. L. Stringer
R. R. Bourassa

ABSTRACT

The problem of nuclear radiation generated currents in signal cables exposed to a radiation field and the change in insulator conductivity caused by radiation have been known and recognized for many years. To date no comprehensive understanding of how the various parameters influence the magnitude and polarity of the signals has been developed. After an analytical model was developed to explain how these currents are generated, experiments were performed in a pulsed TRIGA reactor to evaluate the radiation-induced currents and the induced-conductivity effects on MgO insulated stainless steel coaxial cables. These data are used to estimate the expected readout error from dc sensors located in an environment approximating an FFTF-LMFBR core.

Results of these evaluations for stainless steel coaxial cables insulated with MgO indicate that the readout error, due to a radiation field of 5×10^9 R/hr and 1200 °F, will be equal to:

$$(\%\ \text{error}) = \left| \frac{IR_s}{V} \right| \times 100$$

where I = total radiation-induced current
V = sensor output voltage
R_s = sensor source impedance .

These numerical results should not be applied universally at this point, but rather each individual case must be treated independently because of the large difference in induced currents for different cables.

TABLE OF CONTENTS

LIST OF FIGURES

ESTIMATED READOUT ERRORS PRODUCED BY RADIATION AND TEMPERATURE EFFECTS IN COAXIAL SIGNAL CABLES FOR FFTF

J. L. Stringer
R. R. Bourassa

INTRODUCTION

It is well known that nuclear radiation generates electrical currents in signal cables placed in a nuclear flux.[1-5] It is also known that reactor irradiation increases the conductivity of insulators.[6] The data given in the above references indicate that cable geometry, flux spectrum, cable materials, and many other factors influence the magnitude and polarity of the generated currents. Although many previous investigators have reported on the currents and have partially investigated the phenomena, no complete description of how the various factors influence radiation current generation has been developed. Our initial effort in this direction was the development of a parametric model that gives a qualitative understanding of the mechanisms influencing the generation of the currents.[7] By use of this model as a guide, experimental evaluation of how various cable parameters (e.g., cable geometry, material composition, radiation induced insulator conductivity, radiation flux type, and temperature) influence the polarity and magnitude of the nuclear radiation induced current in cables has started.

Under this program the first effort was to estimate the readout errors that could be produced by radiation-induced signals and radiation-induced conductivity in magnesium-oxide insulated, stainless steel coaxial cables. This report describes the method used to calculate the errors, and presents experimental data used to evaluate the errors

as a function of temperature, radiation field, and sensor source impedance. It also contains graphs of estimated error versus source impedance for a combined temperature and radiation field of 5×10^9 R/hr and 1200 °F.

SUMMARY AND CONCLUSIONS

The equivalent dc circuit for a coaxial cable in a high-radiation high-temperature environment has been developed. Experimentally obtained data for radiation induced current and insulator conductivity have been used to evaluate the cable parameters where 3 ft of cable is in a 5×10^9 R/hr flux zone and 25 ft is in a 10^6 R/hr flux zone with the total (28 ft) cable maintained at 1200 °F.

Two, specific, MgO insulated stainless steel coaxial cables were considered. Their dimensions are 0.250 in. OD, 0.025 in. diam conductor, 0.019 in. sheath; and 0.075 in. OD, 0.025 in. diam conductor, and 0.013 in. sheath. The analysis has shown that the error in a dc sensor voltage at the cable output is given by (% error) = $\left|\frac{IR_s}{V}\right| \times 100$

where I = total radiation induced current
R_s = sensor source impedance (dc)
V = sensor open circuit output voltage (dc).

For the two cables considered, the error is 1% or less when the sensor output voltage is 10 mV or greater; the total induced current is $|1\ \mu A|$ or less, with the sensor source impedance (dc) 100 Ω or less.

When the induced current is assumed to be zero, the insulator shunting effect for a 1% error will allow a sensor source impedance (dc) of 66 kΩ for the larger OD cable, and 39 kΩ for the smaller. The large source impedance values are due to the three order of magnitude improvement in the radiation induced electrical conductivity of the powdered-over solid-insulator material.

DISCUSSION

The general development of a means for making estimates for the influence of radiation-induced currents and radiation-induced conductivity in coaxial signal cables for various source and instrument impedance is given below. Initially, the developed equations are general; however, restrictions on their use are imposed as they are applied to specific cases where only dc sources are considered.

DEVELOPMENT OF EQUIVALENT CIRCUIT FOR CABLE IN A REACTOR CORE

Figure 1 is a circuit diagram of a coaxial cable connecting a voltage source to a measuring instrument. In this diagram the quantities are defined as:

V = Voltage source (volts)

R_s = Source impedance (ohms)

R_T = Terminating impedance (ohms)

R^c_{ij} = resistance/unit length of cable conductor (ohms/unit length)

R^{sh}_{ij} = resistance/unit length of sheath (ohms/unit length)

R^I_{ij} = resistance/unit length of cable insulator (ohms/unit length)

where i and j denote temperature and radiation dose rate environments. Ideally, a signal voltage appearing across R_s and will be measured across R_T. Actually, R^I_{ij} acts as a shunt lowering the measured voltage, with both temperature and radiation effecting the value of R^I_{ij}. In addition to this cause of error, induced currents will be produced in the cable when it is in a radiation environment. The induced currents flow through the shunting resistances causing voltages which are additive to the sensor output to cause an error.

To simplify the problem, we assume a particular temperature and radiation condition representative of the expected FTR

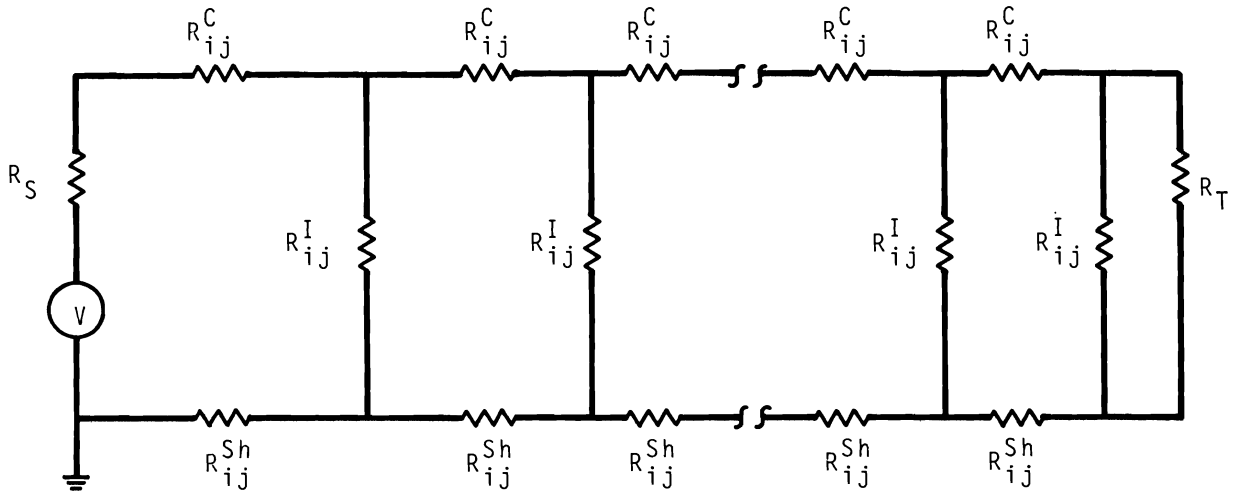

FIGURE 1. A Circuit Diagram of a Coaxial Cable in a Radiation Environment that Connects a Sensor to a Readout Instrument

environment. The environment is depicted in Figure 2. The cable extends 25 ft through a 10^6 R/hr γ-field at a temperature of 1200 °F and extends 3 ft through a reactor core at a temperature of 1200 °F but now in a gamma field of 5×10^9 R/hr. With these assumptions, Figure 1 is simplified to the circuit shown in Figure 3; R_2^I and R_T are replaced by their parallel equivalent, R, where

$$R = \frac{R_2^I \, R_T}{R_2^I + R_T} \quad . \tag{1}$$

The temperature subscript has been dropped since the entire problem is at a constant temperature of 1200 °F. Subscript 1 indicates a γ-field of 5×10^9 R/hr while Subscript 2 indicates 10^6 R/hr. The radiation generated current is represented by the induced current I.

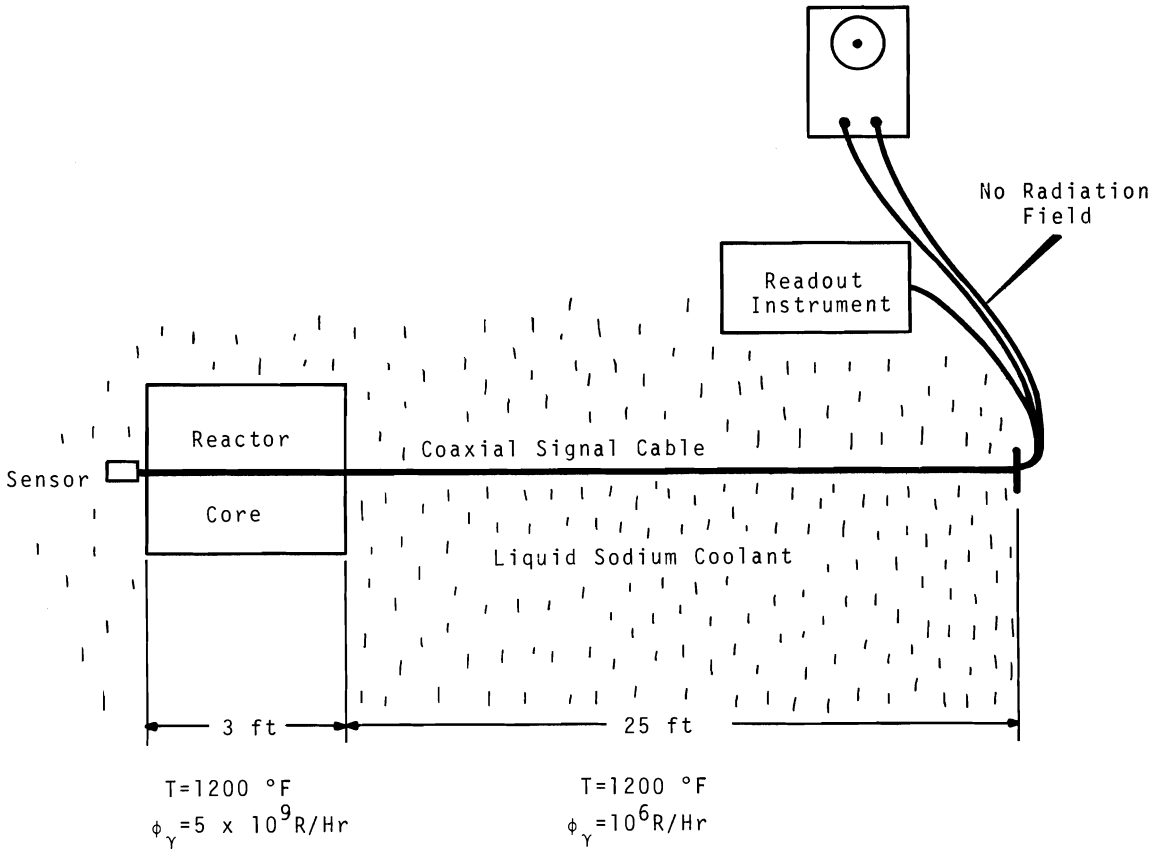

FIGURE 2. Simplified Model of FTR Environment Showing Signal Cable and Sensor Location

The circuit in Figure 3 can be solved for the output voltage V_o where V_o is the voltage measured across R. The solution of this problem is carried out in Appendix A where the expression for the output voltage is given in Equation A-30. The resistances R^c amd R^{sh} will be small compared to other resistances in the problem unless we take $R_s < 10\ \Omega$. Equation A-30 is an exact solution to our model and is given here as

$$V_o = \frac{R_o}{R_o + R_s + R_1^c + R_1^{sh}} \left[V + I\ (R_s + R_1^c + R_1^{sh})\right] \qquad (2)$$

where

$$R_o = \frac{R_1^I\ R}{R_1^I + R} \quad . \qquad (3)$$

The environmental condition will now be used to calculate the values for the resistance terms in Equations (2).

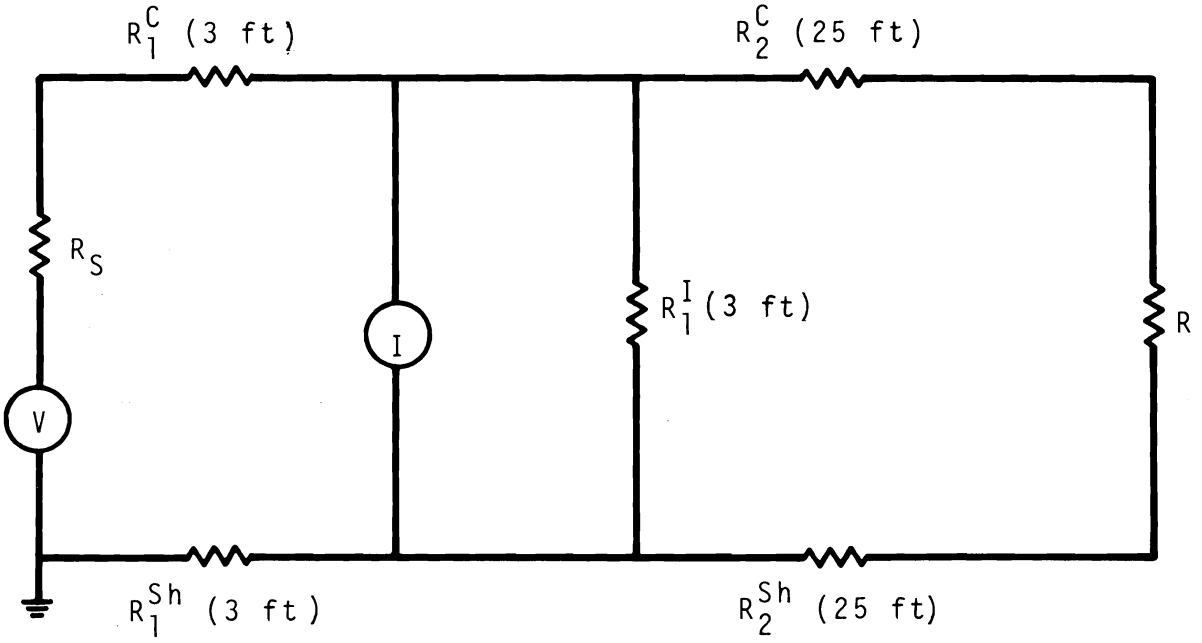

FIGURE 3. Simplified Circuit of a Signal Cable in the FTR

If the cable sheath and conductor are made of a typical stainless steel such as Type 304, the electrical resistance is

$$\rho_{ss} = 69.4\ \mu\Omega\text{-cm (room temperature)} \quad (4)$$

$$\rho_{ss} \simeq 110\ \mu\Omega\text{-cm} = 43.3\ \mu\Omega\text{-in. (1200 °F)} \quad . \quad (5)$$

For this report two cables are considered: one having a 0.250 in. OD, 0.019 in. sheath thickness, and 0.025 in. diam center conductor; the other having a 0.075 in. OD, 0.013 in. sheath, and a 0.024 in. diam center conductor. (These cables are designated as 4E and 3A in our experiments.) Then,

$$R^C = \frac{\rho_{ss}}{\pi a^2} \quad (6)$$

and

$$R^{sh} = \frac{\rho_{ss}}{\pi\left[(\tau_s + b)^2 - b^2\right]} \qquad (7)$$

where

a = conductor radius
b = inner sheath radius
τ_s = sheath thickness .

For cable 4E, a = 0.0125 in., b = 0.106 in., and τ_s = 0.019 in., and for cable 3A, a = 0.012 in., b = 0.025 in., and τ_s = 0.013 in. then

Cable 4E		Cable 3A	
R^c = 0.088 Ω/in.	at 1200 °F	R^c = 0.096 Ω/in.	(8)
R^c = 1.06 Ω/ft		R^c = 1.15 Ω/ft	(9)

Radiation does not change this value significantly, thus,

Cable 4E	Cable 3A	
R_1^c (3 ft) = 3.2 Ω	R_1^c (3 ft) = 3.4 Ω	
R_2^c (25 ft) = 26.5 Ω	R_2^c (25 ft) = 28.8 Ω	(10)

Similarly,

Cable 4E		Cable 3A
R^{sh} = 0.0376 Ω/ft	at 1200 °F	R^{sh} = 0.215 Ω/ft

Thus,

R_1^{sh} (3 ft) = 0.113 Ω, and	R_1^{sh} (3 ft) = 0.643 Ω	
R_2^{sh} (25 ft) = 0.94 Ω	R_2^{sh} (25 ft) = 5.37 Ω	(11)

EVALUATION OF RADIATION INDUCED CONDUCTIVITY INFLUENCE FOR VOLTAGE SOURCE

To evaluate the temperature and radiation effects on the signal cables, experiments were conducted in the ^{60}Co gamma facility at PNL and in the pulsing TRIGA reactor at Washington State University. These experiments were conducted to determine the induced current and insulator conductivity as a function of dose rate and temperature on

specified cables (measurement techniques are detailed in Reference 8). The results presented in Figure 4 show that at a dose rate of 9×10^{10} R/hr* and 1200 °F, the conductivity of the MgO insulation is $\sigma \simeq 8.5 \times 10^{-9}$ $(\Omega\text{-cm})^{-1}$. The results presented are an average of data from four cables, thus are representative of vendor supplied materials. Let G/ℓ be the insulator conductance per unit length of cable. Then,

Cable 4E		Cable 3A
$G/\ell = \frac{2\pi\sigma}{\ln b/a} \simeq 3.0\ \sigma$		$G/\ell = 8.8\ \sigma$
$G/\ell = 2.55 \times 10^{-8}$ $(\Omega\text{-cm})^{-1}$	9×10^{10} R/hr	$G/\ell = 7.5 \times 10^{-8}$ $(\Omega\text{-cm})^{-1}$
$= 7.8 \times 10^{-7}$ $(\Omega\text{-ft})^{-1}$		$= 2.3 \times 10^{-6}$ $(\Omega\text{-ft})^{-1}$
G_1 (3 ft) $= 2.33 \times 10^{-6}$ mhos		G_1 (3 ft) $= 6.85 \times 10^{-6}$ $(\Omega)^{-1}$

and

$R_1^I = \frac{1}{G_1} = 430\ k\Omega$		$R_1^I = \frac{1}{G_1} = 146\ k\Omega$ (12)

To find the conductivity for the conditions of Figure 2, it is assumed that conductivity of MgO is directly proportional to dose rate as indicated for Al_2O_3 by Dau and Davis,[6] and the data of Figure 4 is interpolated to conditions of 5×10^9 R/hr at 1200 °F. The value of R_1^I is

Cable 4E		Cable 3A
$R_1^I = 7.75\ M\Omega$	5×10^9 R/hr	$R_1^I = 2.62\ M\Omega$

At 10^6 R/hr and 1200 °F,

$$\sigma = 1.0 \times 10^{-11}\ (\Omega\text{-cm})^{-1}$$

---

* *It should be noted that the dose rate in the center of the TRIGA core used has not been measured directly with conventional dosimetry techniques. Our value of 9×10^{10} R/hr was obtained by assuming that the insulator conductivity varied linearly with dose rate, and by extrapolating from the known values of conductivity found in the gamma facility at 2.3×10^7 R/hr. The cross checking technique used and literature data all indicate that this a reasonable value.*

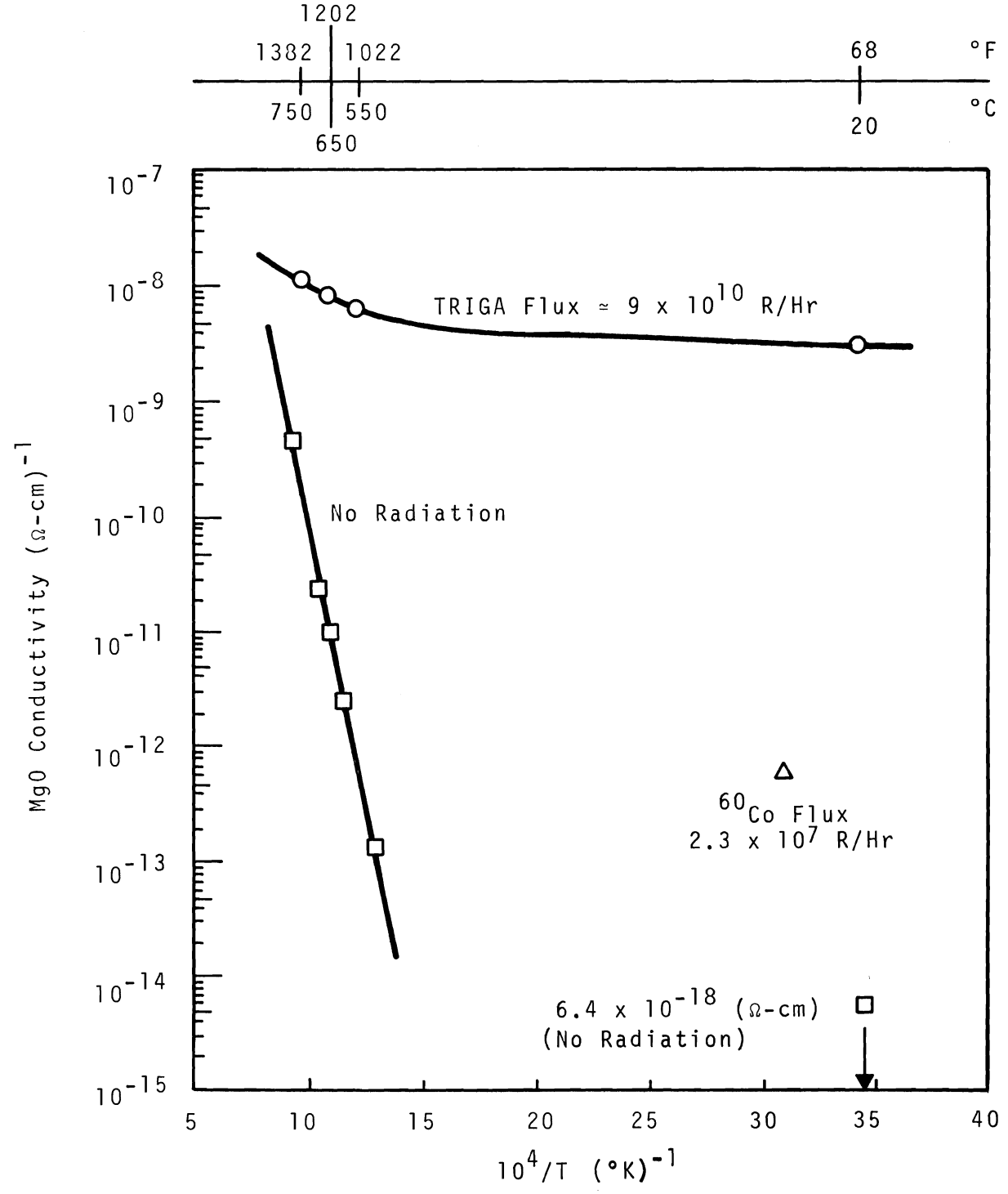

FIGURE 4. A Plot of Conductivity Versus $(T)^{-1}$ for Compacted MgO in Coaxial Cables Showing Temperature and Radiation Dependence

and

Cable 4E	Cable 3A
$G/\ell = 3 \times 10^{-11}$ $(\Omega\text{-cm})^{-1}$	$G/\ell = 8.8 \times 10^{-11}$ $(\Omega\text{-cm})^{-1}$
$= 9.1 \times 10^{-10}$ $(\Omega\text{-ft})^{-1}$	$= 2.7 \times 10^{-9}$ $(\Omega\text{-ft})^{-1}$

or

It should be noted that at this dose rate and temperature (Figure 4), no significant radiation effect is apparent because temperature influences predominate. Thus,

Cable 4E	Cable 3A
G_2 (25 ft) $= 2.28 \times 10^{-8}$ mhos	G_2 (25 ft) $= 6.7 \times 10^{-8}$ mhos

and

$$R_2^I = \frac{1}{G_2} = 44\ M\Omega \qquad R_2^I = \frac{1}{G_2} = 15\ M\Omega \tag{13}$$

If it is assumed that the instrument input impedance, R_T, is infinite, then

Cable 4E	Cable 3A
$R = \dfrac{R_T R_2^I}{R_T + R_2^I} = R_2^I = 44\ M\Omega$	$R = 15\ M\Omega$

and

$$R_o = \frac{R R_1^I}{R_1^I + R} = 6.6\ M\Omega \qquad R_o = 3.9\ M\Omega \tag{14}$$

With the values of the cable resistances calculated, it is easy to show from Equation (2) that

$$\frac{R_o}{R_o + R_s + R_1^c + R_1^{sh}} = 1$$

when

$$R_o \geq 100\ R_s$$

This approximation allows Equation (2) to be simplified to

$$V_o = V + IR_s \tag{15}$$

when values for R_s are limited to

Cable 4E	Cable 3A
$0 \leq R_s \leq 66.0$ kΩ	$0 \leq R_s \leq 39.0$ kΩ

Thus, for an infinite R_T and the stated environmental conditions, the resulting error is given by

$$\% \text{ error} = \left| \frac{V - V_o}{V} \right| \times 100 = \left| \frac{I R_s}{V} \right| \times 100 \quad . \qquad (16)$$

If the induced current, I, is zero, then the error from a voltage source [Equation (2)] will be $\leq 1\%$ unless $R_s > 66.0$ kΩ for 4E and > 39.0 kΩ for 3A. The above exercise indicates that induced conductivity in MgO insulated cables will not be a problem if the sensor source impedance is less than the calculated limits with the stated environmental conditions.

EVALUATION OF RADIATION INDUCED CURRENT INFLUENCE FOR VOLTAGE SOURCE

The magnitude of the current, I, induced in the cable by radiation will be influenced by a number of factors discussed in detail in Reference 7. A realistic estimate (based on our experiments) for 3 ft of cable at 5×10^9 R/hr is

4E	3A
$I = -1$ μA	$I = -0.5$ μA

Use of these values for the induced current in Equation (16) gives the error values (Figures 5 and 6) for different values of sensor output voltage, V, as a function of R_s.

Percent error below 100 means that the measured voltage is less than the generated voltage by the percent specified. Percent error above 100 means the measured voltage is of opposite polarity to the generated voltage and has a magnitude given by the percentage over 100. These results should be applied carefully because if the induced current doubles, the percent error doubles. Each case requires individual attention.

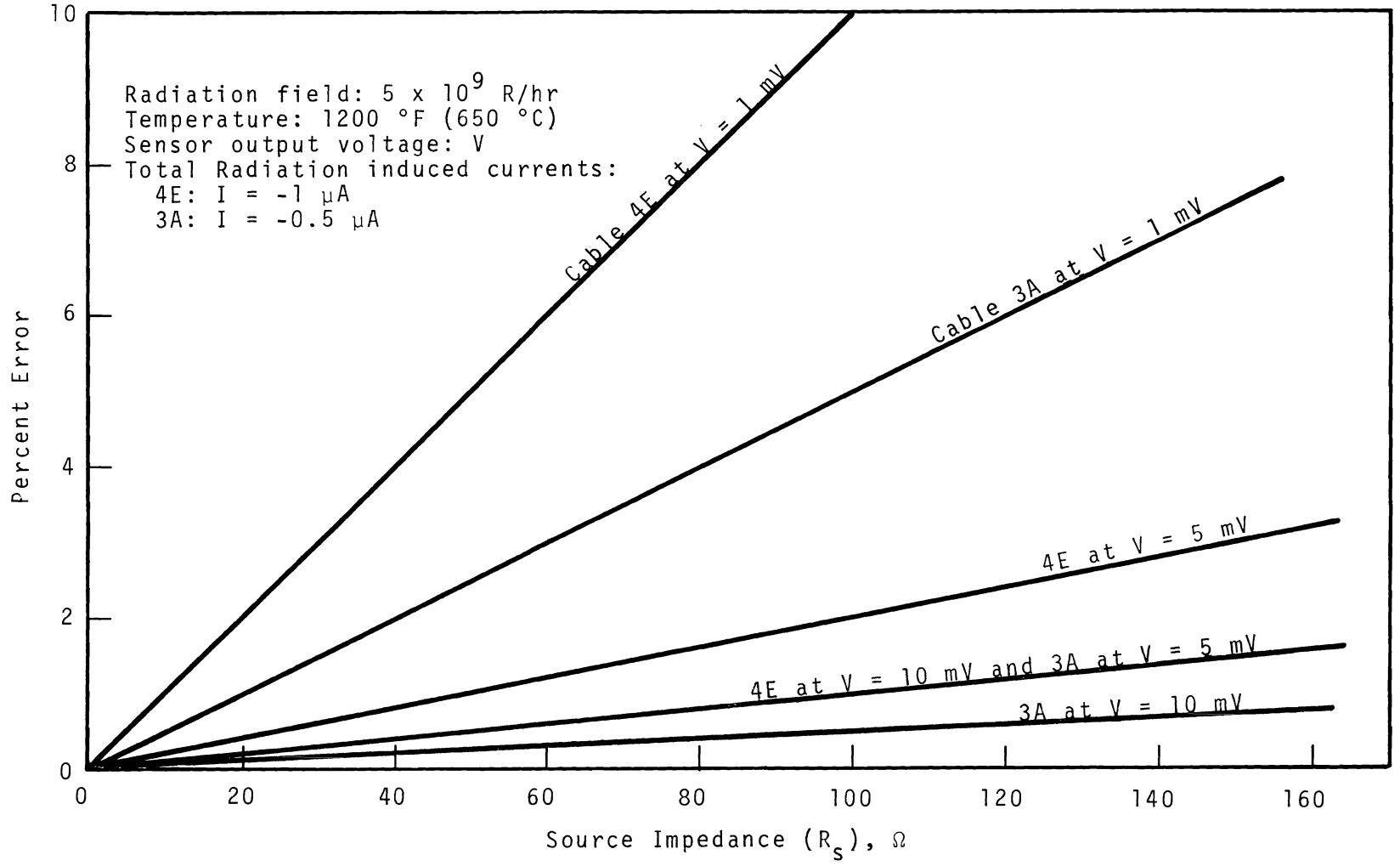

FIGURE 5. Estimated Percent Error Versus Source Impedance for Typical Coaxial Cables

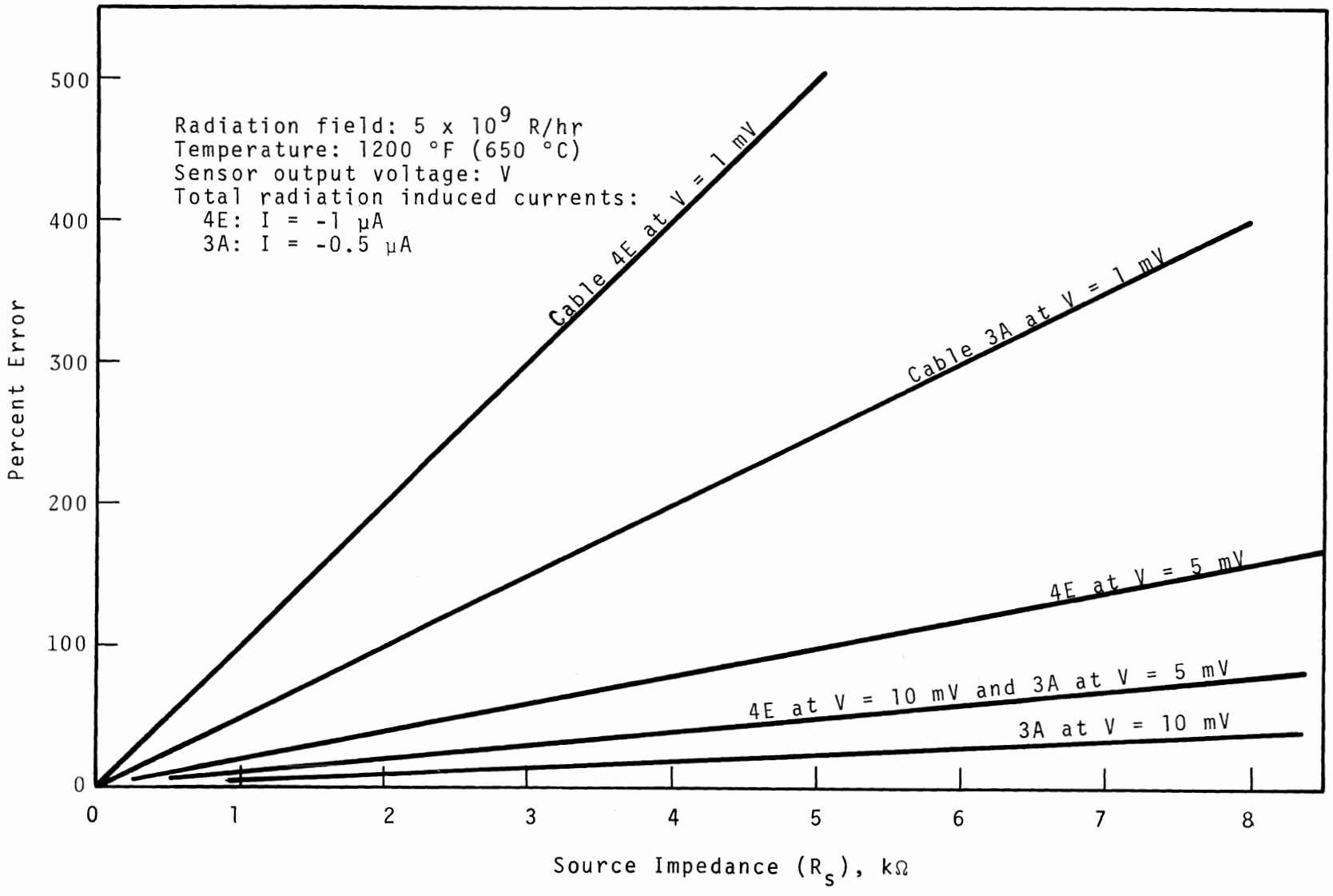

FIGURE 6. Estimated Percent Error Versus Source Impedance for Typical Coaxial Cables

RADIATION AND TEMPERATURE INFLUENCE WHEN SENSOR IS A CURRENT SOURCE

The equations describing the influence of temperature and radiation on a coaxial cable used to transmit a signal from a current source sensor (e.g., an ion chamber) to a readout device are developed in Appendix A. The pertinent equation [Equation (A-36)] is repeated below.

$$i_o = \frac{R_s}{R_o + R_s + R_1^c + R_1^{sh}} \left(i_i + I \left\{ 1 + \frac{R_1^c}{R_s} + \frac{R_1^{sh}}{R_s} \right\} \right) \qquad (17)$$

where

i_o = output current

i_i = input current from sensor

$R_{to} = R_2^c + R + R_2^{sh}$

$\frac{1}{R_o} = \frac{1}{R_1^I} + \frac{1}{R_{to}}$ [Equation (A-19)]

The other terms are the same as defined in Figure 3. By using values of the resistances for the cable described previously, it is evident that $R_{to} = R$ because, typically, $R \geq 1$ kΩ for a current meter. Thus,

$$\frac{1}{R_o} = \frac{1}{R_1^I} = \frac{1}{R} \approx \frac{1}{R} \qquad (18)$$

or

$$R_o = R$$

because $R_1^I >> R$ is a necessary condition for measuring a current. Also, $R_s >> R$, R_1^c, R_1^{sh} so that

$$i_o = i_i + I \quad . \qquad (19)$$

From this analysis we see that the error consists of the addition of the induced current. Presently, there is insufficient data available to accurately predict the magnitude and

polarity of the induced current for every cable that could be used. For the two examples used here, a sensor whose current output is 100 times the maximum induced current will have an insignificant error at the cable output.

COMMENTS

This analysis gives an estimate of the expected readout error for sensors located in an FFTF-type core and, as such, should prove very useful to efforts directed toward sensor development. Although the examples used in the report are specific, considerable experimental data from the program have been given so that reasonable error estimates can be made for other conditions.

Data for the radiation-induced insulator electrical conductivity given in Reference (6) for Al_2O_3 as a solid insulator would have an extrapolated value of 7×10^{-7} $(ohm\text{-}cm)^{-1}$ at 5×10^{9} R/hr. The data given in this report for powdered MgO and extrapolated to 5×10^{9} R/hr give a value of 4.4×10^{-10} $(ohm\text{-}cm)^{-1}$. The ratio of the Al_2O_3 solid to the MgO powder is 1.6×10^{3}. If it were not for this improvement in the radiation performance, the source resistance limit for the two cables (4E and 3A) would be 43 Ω and 25 Ω, respectively, and the output error would be primarily a function of the radiation-induced cable shunting resistance rather than the induced current.

Certain assumptions were made in making the estimates in this report. These assumptions are:

- The radiation-induced conductivity changes linearly at 10^{10} R/hr, as it does at 10^{7} R/hr.
- The magnitude of the cable currents generated is linearly proportional to the radiation flux.

Many good reasons can be given why these assumptions are valid; however, experiments (which are planned) are needed to provide the necessary verification. In addition, experimental evaluation of the variation of current magnitude and polarity as a function of cable size and neutron to gamma flux ratio is needed so that more general error estimates can be made. For example, altering the neutron to gamma flux ratio for Cable 3A caused the polarity of the total induced current to change from positive to negative. Sufficient data are not available to quantize this effect.

ACKNOWLEDGEMENTS

The authors gratefully acknowledge the exceptional effort by R. D. Breneman for his assistance in assembling and conducting the experimental work. Our thanks are also extended to the staff of the Nuclear Reactor Laboratory at Washington State University for their cooperation. The assistance of Dr. Gary J. Dau in preparing this manuscript is also acknowledged.

REFERENCES

1. F. D. Terry. Effects of Transient Nuclear Radiation on Transducers and Electrical Cables, IDO-16914. Idaho Operations Office, Idaho Falls, Idaho, November 1963.

2. F. D. Terry, R. L. Kindred, and S. D. Anderson. Transient Nuclear Radiation Effects on Transducer Devices and Electrical Cables, IDO-17103. Idaho Operations Office, Idaho Falls, Idaho, November 1965.

3. W. L. Bunch and M. R. Wood. Boron-11 Neutron Flux Monitors: Interim Report, BNWL-64. Pacific Northwest Laboratory, Richland, Washington, April 1965.

4. C. N. Jackson, Jr. ^{11}B-Beta Current Thermal Neutron Flux Detector, BNWL-395. Pacific Northwest Laboratory, Richland, Washington, April 1967.

5. J. W. Hilborn. "Self Powered Neutron Detectors for Reactor Flux Monitoring," Nucleonics, vol. 22, no. 2, p 69. February 1964.

6. G. J. Dau and M. V. Davis. "Gamma Induced Electrical Conductivity in Alumina," Nucl. Sci. and Engr. vol. 25, pp. 223-226. 1966.

7. J. L. Stringer and R. R. Bourassa. Nuclear Radiation Induced Currents in Coaxial Signal Cables, BNWL-749. Pacific Northwest Laboratory, Richland, Washington, June 1968.

8. J. L. Stringer. Unpublished Data. Radiation Induced Current and Electrical Conductivity Measurement Techniques. Pacific Northwest Laboratory, Richland, Washington. (Preliminary Report)

APPENDIX A

DEVELOPMENT OF CABLE CIRCUIT EQUATIONS

APPENDIX A

DEVELOPMENT OF CABLE CIRCUIT EQUATIONS

VOLTAGE SOURCE CASE

To use node equations, we replace V and R_s with the equivalent current source. Call the voltage between ground and a, V_a, and the current through V, I_1 (See Figure 7).

The $V_a = V - I_1 R_s$ (A-1)

Thus,

$$I_1 = \frac{V}{R_s} - \frac{V_a}{R_s} \quad \text{(A-2)}$$

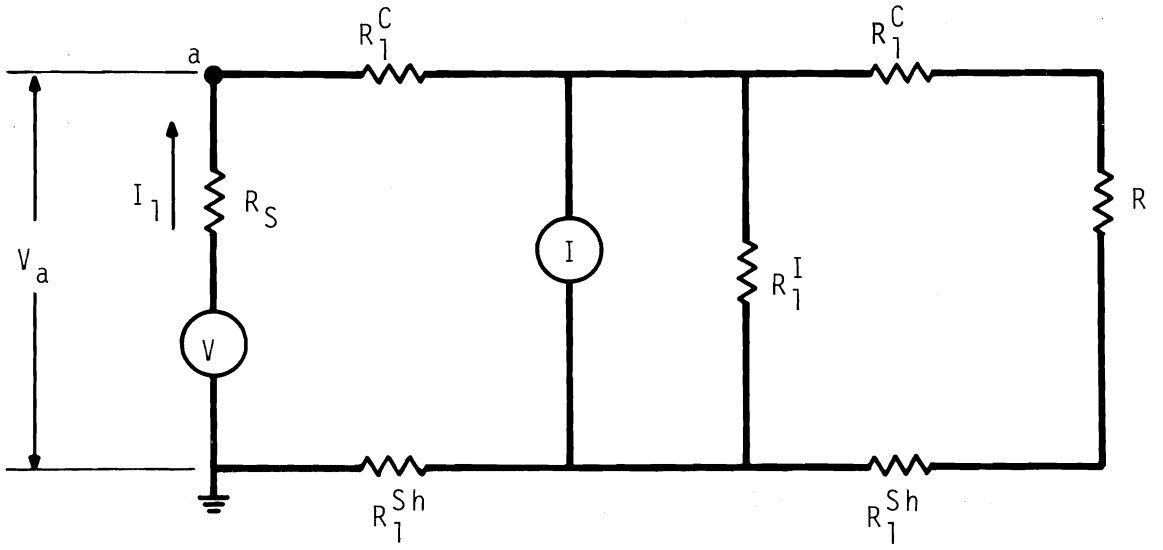

FIGURE 7. Equivalent Circuit of a Coaxial Cable

Replacing V and R_s in terms of currents allows us to write node equations. Note that voltages V_a, V_b, and V_c and currents i, i_2, i_3, i_4, i_5, and i_6 are defined as shown in Figure 8. We now write the node equations, putting them in terms of V_a, V_b, and V_c.

$$i_3 = i_2 + i_1 \tag{A-3}$$

$$i_1 = i_5 + i_4 - I \tag{A-4}$$

$$i_5 + i_4 = I + i_6 \tag{A-5}$$

$$i_1 = \frac{V_a - V_b}{R_s} \tag{A-6}$$

$$i_2 = \frac{V_a}{R_s} \tag{A-7}$$

$$i_3 = \frac{V}{R_s} \tag{A-8}$$

$$i_4 = \frac{V_b - V_c}{R_2^c + R + R_2^{sh}} \tag{A-9}$$

$$i_5 = \frac{V_b - V_c}{R_1^I} \tag{A-10}$$

$$i_6 = \frac{V_c}{R_1^{sh}} \tag{A-11}$$

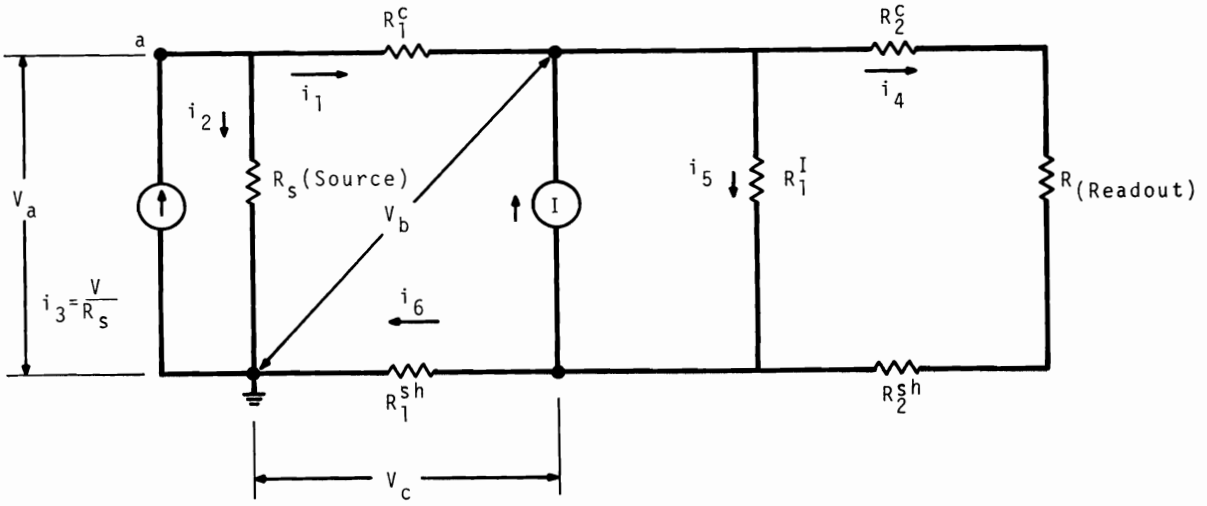

FIGURE 8. Circuit from Which Node Equations Are Written

Thus,

$$\frac{V}{R_s} = \frac{V_a}{R_s} + \frac{V_a - V_b}{R_1^c} \tag{A-12}$$

$$\frac{V_a - V_b}{R_1^c} + I = \frac{V_b - V_c}{R_1^I} + \frac{V_b - V_c}{R_2^c + R + R_2^{sh}} \tag{A-13}$$

$$\frac{V_c}{R_1^{sh}} + I = \frac{V_b - V_c}{R_1^I} + \frac{V_b - V_c}{R_2^c + R + R_2^{sh}} \tag{A-14}$$

Let

$$R_{to} = R_2^c + R + R_2^{sh} \tag{A-15}$$

$$\frac{V}{R_s} = V_a \left(\frac{1}{R_s} + \frac{1}{R_1^c}\right) - \frac{V_b}{R_1^c} \tag{A-16}$$

$$I = -\frac{V_a}{R_1^c} + V_b \left(\frac{1}{R_1^I} + \frac{1}{R_{to}} + \frac{1}{R_1^c}\right) - V_c \left(\frac{1}{R_1^I} + \frac{1}{R_{to}}\right) \tag{A-17}$$

$$I = +V_b \left(\frac{1}{R_1^I} + \frac{1}{R_{to}}\right) - V_c \left(\frac{1}{R_1^I} + \frac{1}{R_{to}} + \frac{1}{R_1^{sh}}\right) \tag{A-18}$$

Let

$$\frac{1}{R_o} = \frac{1}{R_1^I} + \frac{1}{R_{to}} \tag{A-19}$$

$$V_b = \frac{\begin{vmatrix} \left(\frac{1}{R_s} + \frac{1}{R_1^c}\right) & \frac{V}{R_s} & 0 \\ -\frac{1}{R_1^c} & I & -\frac{1}{R_o} \\ 0 & I & -\left(\frac{1}{R_o} + \frac{1}{R_1^{sh}}\right) \end{vmatrix}}{\begin{vmatrix} \left(\frac{1}{R_s} + \frac{1}{R_1^c}\right) & -\frac{1}{R_1^c} & 0 \\ -\frac{1}{R_1^c} & \left(\frac{1}{R_o} + \frac{1}{R_1^c}\right) & -\frac{1}{R_o} \\ 0 & \frac{1}{R_o} & -\left(\frac{1}{R_o} + \frac{1}{R_1^{sh}}\right) \end{vmatrix}} \qquad \text{(A-20)}$$

$$V_b = \frac{\left(\frac{1}{R_s} + \frac{1}{R_1^c}\right)\left[-I\left(\frac{1}{R_o} + \frac{1}{R_1^{sh}}\right) + I\frac{1}{R_o}\right] - \frac{V}{R_s R_1^c R_1^{sh}} - \frac{V}{R_s R_1^c R_1^{sh}}}{\left\{-\left(\frac{1}{R_s} + \frac{1}{R_1^c}\right)\left[\frac{1}{R_o}\frac{1}{R_1^{sh}} + \frac{1}{R_1^c}\frac{1}{R_o} + \frac{1}{R_1^c}\frac{1}{R_1^{sh}}\right] + \frac{1}{(R_c^1)^2}\left(\frac{1}{R_o} + \frac{1}{R_1^{sh}}\right)\right\}}$$

Call the denominator [den]. (A-22)

$$V_c = \frac{\begin{vmatrix} \left(\frac{1}{R_s} + \frac{1}{R_1^c}\right) & -\frac{1}{R_1^c} & \frac{V}{R_s} \\ -\frac{1}{R_1^c} & \left(\frac{1}{R_o} + \frac{1}{R_1^c}\right) & I \\ 0 & \frac{1}{R_o} & I \end{vmatrix}}{[\text{den}]} \qquad \text{(A-23)}$$

$$V_c = \frac{\left(\frac{1}{R_s} + \frac{1}{R_1^c}\right)\left[I\left(\frac{1}{R_o} + \frac{1}{R_1^c}\right) - I\,\frac{1}{R_o}\right] - I\left(\frac{1}{R_1^c}\right)^2 - \frac{V}{R_s\ R_o\ R_1^c}}{[\text{den}]} \quad \text{(A-24)}$$

$$V_b - V_c = \frac{-I\left(\frac{1}{R_s} + \frac{1}{R_1^c}\right)\left(\frac{1}{R_1^{sh}} + \frac{1}{R_1^c}\right) + I\left(\frac{1}{R_1^c}\right)^2 - \frac{V}{R_s\ R_1^c\ R_1^{sh}}}{[\text{den}]} \quad \text{(A-25)}$$

$$i_4 = \frac{-I\left(\frac{1}{R_s}\frac{1}{R_1^{sh}} + \frac{1}{R_1^c}\frac{1}{R_1^{sh}} + \frac{1}{R_s}\frac{1}{R_1^c} - \frac{V}{R_s\ R_1^c\ R_1^{sh}}\right.}{R_{to}\ [\text{den}]} \quad \text{(A-26)}$$

$$i_4 = \frac{V_b - V_c}{R_{to}} = \frac{V_b - V_c}{R} \quad \text{because } R >> R_2^{sh},\ R_2^c \quad \text{(A-27)}$$

$$V_o = i_4 R = V_b - V_c \quad \text{(A-28)}$$

$$V_o = \frac{-I\left[\frac{1}{R_s\ R_1^{sh}} + \frac{1}{R_1^c\ R_1^{sh}} + \frac{1}{R_1^c\ R_s}\right] - \frac{V}{R_1^c\ R_s\ R_1^{sh}}}{\left(\frac{1}{R_1^c}\right)^2\left(\frac{1}{R_o} + \frac{1}{R_1^{sh}}\right) - \left(\frac{1}{R_s} + \frac{1}{R_1^c}\right)\left[\frac{1}{R_o}\left(\frac{1}{R_1^c} + \frac{1}{R_1^{sh}}\right) + \frac{1}{R_1^c\ R_1^{sh}}\right.} \quad \text{(A-29)}$$

After simplifying the denominator, the above equation reduces to

$$V_o = \left[\frac{I\ R_s + R_1^{sh} + R_1^c}{R_o + R_s + R_1^c + R_1^{sh}} + \frac{V}{R_o + R_s + R_1^c + R_1^{sh}}\right] R_o \quad \text{(A-30)}$$

By analyzing the order of magnitude of the resistances expected in a typical cable, it is apparent that

$R_o \approx R_1^I >> R_s + R_1^c + R_1^{sh}$ so that

$R_o + R_s + R_1^c + R_1^{sh} \approx R_o$.

Thus, Equation (A-30) can be reduced to

$$V_o = I\left(R_s + R_1^{sh} + R_1^c\right) + V \text{ (Voltage source)} \quad \text{(A-31)}$$

CURRENT SOURCE CASE

By considering a sensor (e.g., an ion chamber) that is a current source, the output and sensor input will be in terms of an electrical current. With this in mind, it is possible to see (Figure 8) that the output current, i_o, is

$$i_o = i_4 + i_5 = \frac{V_o}{R_o} \tag{A-32}$$

where

$$R_o = \frac{R_1^I \left(R + R_2^c + R_2^{sh}\right)}{R_1^I + R + R_2^c + R_2^{sh}} \tag{A-33}$$

The sensor input current, i_i, is (from Figure 8)

$$i_i = i_3 = \frac{V}{R_s} \tag{A-34}$$

If both sides of Equation (A-30) are divided by R_s and the result simplified [noting Equation (A-32)],

$$i_o = \left[\frac{R_s}{R_o + R_s + R_1^{sh} + R_1^c}\right]\left[I\left\{1 + \frac{1}{R_s}\left(R_1^c + R_1^{sh}\right)\right\} + i_i\right] \tag{A-35}$$

The circuit can be simplified by introducing the resistance R_o [defined in Equation (A-33)] as shown in Figure 9.

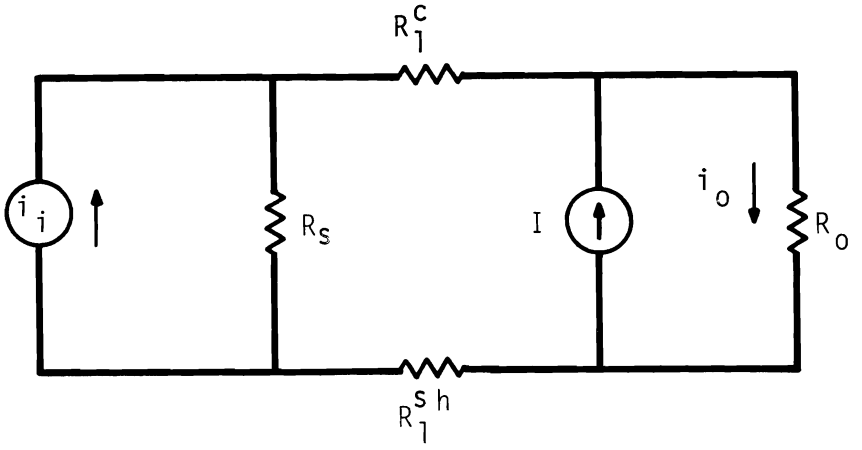

FIGURE 9. Simplified Equivalent Circuit for Current Source

Then

$$i_o = \left(\frac{R_s}{R_o + R_s + R_1^c + R_1^{sh}}\right) i_i + \left(\frac{R_s + R_1^c + R_1^{sh}}{R_o + R_s + R_1^c + R_1^{sh}}\right) I$$

$$= \left(\frac{R_s}{R_o + R_s + R_1^c + R_1^{sh}}\right) \left(i_i + I \left\{1 + \frac{R_1^c}{R_s} + \frac{R_1^{sh}}{R_s}\right\}\right) \qquad \text{(A-36)}$$

DISTRIBUTION

No. of Copies

OFFSITE

1 AEC Chicago Patent Group

G. H. Lee, Chief

30 AEC Division of Reactor Development and Technology

M. Shaw, Director, RDT
Asst Dir for Nuclear Safety
Analysis & Evaluation Br, RDT:NS
Environmental & Sanitary Engrg Br, RDT:NS
Research & Development Br, RDT:NS
Asst Dir for Plant Engrg, RDT
Facilities Br, RDT:PE
Components Br, RDT:PE
Instrumentation & Control Br, RDT:PE
Liquid Metal Systems Br, RDT:PE
Asst Dir for Program Analysis, RDT
Asst Dir for Project Mgmt, RDT
Liquid Metals Projects Br, RDT:PM
FFTF Project Manager, RDT:PM (3)
Asst Dir for Reactor Engrg, RDT
Control Mechanisms Br, RDT:RE
Core Design Br, RDT:RE (2)
Fuel Engineering Br, RDT:RE
Fuel Handling Br, RDT:RE
Reactor Vessels Br, RDT:RE
Asst Dir for Reactor Tech, RDT
Coolant Chemistry Br, RDT:RT
Fuel Recycle Br, RDT:RT
Fuels & Materials Br, RDT:RT
Reactor Physics Br, RDT:RT
Special Technology Br, RDT:RT
Asst Dir for Engrg Standards, RDT

228 AEC Division of Technical Information Extension

1 AEC Idaho Operations Office
Nuclear Technology Division

C. W. Bills, Director

1 AEC San Francisco Operations Office
Director, Reactor Division

4 AEC Site Representatives

Argonne National Laboratory
Atomics International
Atomic Power Development Associates
General Electric Co., Sunnyvale, California

3 Argonne National Laboratory

R. A. Jaross
LMFBF Program Office
N. J. Swanson

2 Atomic Energy of Canada, Limited
Chalk River Laboratory, Ontario, Canada

J. W. Hilborn
A. Pearson

2 Atomic Power Development Associates

Document Librarian
A. G. Hosler

7 Atomics International

D. J. Cockeram (5)

Liquid Metal Engineering Center

J. J. Droher (2)

2 Babcock & Wilcox Co. (AEC)
Atomic Energy Division

S. H. Esleeck
G. B. Garton

5 Bechtel Corporation

J. J. Teachnor, Project Administrator, FFTF

1 BNW Representative

N. A. Hill (ZPR III)

1 Combustion Engineering Inc. (AEC)
1000 MWe Follow-On Study

W. P. Staker, Project Manager

5 General Electric Co.
Advanced Products Operation
Sunnyvale, California

Karl Cohen (3)
Bertram Wolfe

Nuclear Systems Program

D. H. Ahmann

2 Gulf General Atomic Inc. (AEC)
General Atomic Division
D. Coburn

1 Idaho Nuclear Corporation
D. R. deBoisblanc

1 Oak Ridge National Laboratory
W. O. Harms

1 Stanford University
Nuclear Division
Division of Mechanical Engineering
R. Sher

1 United Nuclear Corporation
Research and Engineering Center
R. F. DeAngelis

1 University of Arizona
Nuclear Engineering Department
Tucson, Arizona
M. V. Davis

1 University of Oklahoma
Department of Physics
Norman, Oklahoma
R. R. Bourassa

2 University of Washington
Nuclear Engineering Department
Seattle, Washington
A. L Babb
M. A. Robkin

2 Washington State University
Nuclear Reactor Laboratory
Pullman, Washington
H. Dodgen
H. Stern

10 Westinghouse Electric Corp.
Atomic Power Division
Advanced Reactor Systems
J. C. R. Kelly

ONSITE-HANFORD

1 AEC Chicago Patent Group

R. K. Sharp (Richland)

4 AEC RDT Site Representative

P. G. Holsted

3 AEC Richland Operations Office

J. M. Shivley

3 Battelle Memorial Institute

1 Bechtel Corporation

D. H. Weiss (Richland)

1 Westinghouse Electric Corp.

R. Strzelecki (Richland)

98 Battelle-Northwest

S. O. Arneson
E. R. Astley
J. M. Batch
A. L. Bement, Jr.
C. A. Bennett
R. A. Bennett
T. R. Billeter
B. B. Brenden
D. P. Brown
W. L. Bunch
J. R. Carrell
W. E. Cawley
W. L. Chase
T. T. Claudson
J. C. Cochran
D. L. Condotta
R. R. Cone
T. Crocker
G. M. Dalen
W. Dalos
G. J. Dau (20)
J. M. Davidson
E. A. Evans
L. M. Finch
R. L. Gordon
R. E. Heineman
N. C. Hoitink
P. L. Hofmann
C. N. Jackson
J. L. Jackson
E. M. Johnston
D. D. Lanning
C. W. Lindenmeier
C. E. Love
B. Mann
W. B. McDonald
J. S. McMahon
V. I. Neeley
H. N. Pederson
R. E. Peterson
N. S. Porter
W. E. Roake
F. H. Shadel
D. E. Simpson
C. R. F. Smith
W. G. Spear
R. J. Squires
J. L. Stringer (5)
G. H. Strong
C. D. Swanson
D. C. Thompson
J. C. Tobin
R. W. Truitt
R. C. Walker
J. H. Westsik
W. E. Wilson
M. R. Wood
D. C. Worlton
FFTF Files (10)
Technical Information (5)
Technical Publications (2)